



A type IV functional response with different shapes in a predator–prey model



Merlin C. Köhnke^{a,*}, Ivo Siekmann^b, Hiromi Seno^c, Horst Malchow^a

^a Institute of Mathematics, School of Mathematics/Computer Science, Osnabrück University, Germany

^b Liverpool John Moores University, Department of Applied Mathematics, Liverpool L3 3AF, United Kingdom

^c Research Center for Pure and Applied Mathematics, Graduate School of Information Sciences, Tohoku University, Aramaki-Aza-Aoba 6-3-09, Aoba-ku, Sendai 980-8579, Japan

ARTICLE INFO

Article history:

Received 4 March 2020

Revised 23 June 2020

Accepted 18 July 2020

Available online 28 July 2020

Keywords:

Type IV functional response
Dome-shaped functional response
Group defense

ABSTRACT

Group defense is a phenomenon that occurs in many predator–prey systems. Different functional responses with substantially different properties representing such a mechanism exist. Here, we develop a functional response using timescale separation. A prey-dependent catch rate represents the group defense. The resulting functional response contains a single parameter that controls whether the group defense functional response is saturating or dome-shaped. Based on that, we show that the catch rate must not increase monotonically with increasing prey density to lead to a dome-shaped functional response. We apply bifurcation analysis to show that non-monotonic group defense is usually more successful. However, we also find parameter regions in which a paradox occurs. In this case, higher group defense can give rise to a stable limit cycle, while for lower values, the predator would go extinct. The study does not only provide valuable insight on how to include functional responses representing group defense in mathematical models, but it also clarifies under which circumstances the usage of different functional responses is appropriate.

© 2020 Elsevier Ltd. All rights reserved.

1. Introduction

Predation is a ubiquitous interaction in ecological communities (Allan, 1995). The dynamics of mathematical models describing predator–prey relationships depend critically on the functional response (Abrams and Ginzburg, 2000; Gross et al., 2004; Aldebert et al., 2016). The most commonly used functional responses rely on the work of Holling (1959, 1961). These are categorized as Holling type I, II, and III functional responses. However, a wide range of other functional responses exist as well, and even though the shape of the functional response is similar (for instance, the Holling type II and the Ivlev functional response (Ivlev, 1961)), the dynamics may change qualitatively (Aldebert et al., 2016). This phenomenon is called structural sensitivity.

In this study, we will focus on a mathematical predator–prey model incorporating a group defense of the prey. It is well known that some prey species adapt to predation and can develop different avoidance or defense strategies (Jeschke, 2006). Some bacteria, for instance, produce toxins that may be lethal for eukaryotic predators (Lainhart et al., 2009). However, avoidance strategies

such as flight, freezing (Blanchard et al., 1986), using refuge areas, or a combination of these (Blanchard et al., 1990) usually do not have a direct negative impact on the predator population (Edmunds, 1974). Instead, decreasing the attack success due to predator confusion can reduce the predation without harming the predator (Allee, 1958; Jeschke and Tollrian, 2005). For instance, moose use intimidation of wolves as a non-harmful defense strategy (Caro, 2005). Another example is given by plankton sensing predator kairomones leading to morphological changes, which is a successful defense strategy against size-selective predators (Lass and Spaak, 2003). Besides, many species warn conspecifics of the group using alarm signals (Klump and Shalter, 1984). Such a swarming effect often occurs in social populations (Tener, 1965; Líznavá and Pekár, 2013).

In mathematical models, anti-predator defense strategies have often been incorporated by a potentially adaptive decrease in handling time, an increase in attack rates, or a combination of these two (Jeschke and Tollrian, 2000; Líznavá and Pekár, 2013; Köhnke, 2019). However, as many of the defense mechanisms depend on the population size of the prey (Krams et al., 2009), often also a dome-shaped functional response is used. The characteristic feature of a dome-shaped functional response is that the consumed prey for a particular prey density has a maximum at finite prey densities. Different experiments have confirmed the

* Corresponding author.

E-mail address: merlin.koehnke@uos.de (M.C. Köhnke).

dome-shape, such as Pekár (2005), as well as Líznavá and Pekár (2013). However, group defense is likely to be present in many systems, although not indicated by the functional response (Jeschke and Tollrian, 2005). Even though, not in his classical paper about functional responses (Holling (1959)), in Holling (1961), already Holling has proposed four functional responses, one of them incorporating a swarming effect leading to a dome-shaped functional response. Hence, this is often referred to as a Holling type IV functional response (Huang and Xiao, 2004; Lian and Xu, 2009; Wang et al., 2009). However, classically only type I, II, and III are referred to as Holling types. To avoid confusion, we will stick to the term type IV functional response throughout this paper.

Different expressions exist for such a type IV functional response (Tostowaryk, 1972; Fujii et al., 1986; Líznavá and Pekár, 2013). Particularly some studies use a type IV functional response with a square prey dependence in the denominator but without any linear dependence (Zhang et al., 2006; Baek, 2010). These usually have a form similar to

$$f_{IV}(U) = \frac{U}{1 + U^2}. \quad (1)$$

This form was originally proposed by Sokol and Howell (1981) as a simplification of a functional response that also incorporates a linear prey dependence in the denominator. Such kind of response is sometimes referred to as Monod-Haldane functional response (Andrews, 1968) and is commonly used as well (Edwards, 1970; Chen, 2004; Upadhyay and Raw, 2011). Collings (1997) derived a similar functional response resulting from the assumption that searching efficacy and handling time are decreasing and increasing with prey density, respectively.

In Section 2, we develop a functional response based on a quasi-steady-state assumption. Applying quasi-steady-state assumptions is a powerful tool ranging back to Bodenstein (1913). It can help to significantly simplify dynamical systems using the idea that processes described by the dynamical system happen on different timescales (Shoffner and Schnell, 2017). We will show that, if the catch rate is monotonically increasing with prey density, the resulting functional response will be saturating. Otherwise, the functional response can be dome-shaped. We will analyze the rather general model analytically before we introduce a functional response incorporating a group defense in Section 3. The shape of this functional response can be varied using a single parameter. We will treat this model analytically and with bifurcation analysis to show that the group defense can drive the predator to extinction. However, we will also show that for a small parameter region, a paradox occurs.

2. General model

We start with developing a predator-prey model of the form

$$\frac{dU}{dT} = \Phi(U) - f(U)V, \quad U(0) = U_0, \quad (2a)$$

$$\frac{dV}{dT} = Q(f(U)V) - mV, \quad V(0) = V_0 \quad (2b)$$

with

$$\Phi(0) = \Phi(K) = 0, \quad \Phi'(K) < 0. \quad (2c)$$

with all parameters being positive. Here, K represents the carrying capacity of the prey population. The prey U grows according to the function $\Phi(U)$ in absence of the predator V . This function has at least two stationary states, the extinction, and the carrying capacity. Furthermore, the carrying capacity is stable in absence of the predator. We model the mortality of the predator with a linear term. The term $f(U)$ is the functional response, i.e., how the number of predated prey per unit time of one average predator varies with changing densities. Note that we are interested in group

defense and thus assume that the functional response is only affected by the prey density. The function $Q(f(U)V)$ represents the biomass production of V due to predation, i.e., the numerical response.

To develop the functional response, we assume that the predator can be divided into two separate states, searching and handling, i.e., $V = S + H$. Note that an alternative approach to develop a functional response is by argumentations on time budgets of the prey. An example regarding group behavior is given by Braza (2012). The dynamics of the subpopulations are given by

$$\frac{dS}{dT} = -\beta g(U)S + \gamma H, \quad S(0) = S_0, \quad g(0) = 0, \quad (3a)$$

$$\frac{dH}{dT} = \beta g(U)S - \gamma H, \quad H(0) = H_0. \quad (3b)$$

This approach also allows for the derivation of a Holling type II functional response (Diekmann et al., 2012). Note that we neglect birth and death processes here, assuming that they happen on a much slower timescale (for a discussion on the validity of such a timescale separation see Appendix A). Hence, $V = S + H = \text{const.}$ holds for this timescale. Searching individuals turn into handling individuals by capturing prey with a rate β depending on the function $g(U)$. The function $g(U)$ represents the rate of successful catch and kill per searching predator, while β represents the search rate. Throughout the manuscript, we will refer to $g(U)$ as *catch rate*. Note that in this interpretation, handling individuals are all individuals that are not actively searching for prey, for instance, handling prey or digesting it. After some handling time $\tau = \gamma^{-1}$, handling individuals turn back into searching individuals.

Applying time-scale separation, we can find a quasi-stationary solution for the searching subpopulation

$$S^* = \frac{\gamma V}{\beta g(U) + \gamma}. \quad (4)$$

Now, we assume that predation depends only on searching individuals which allows us to introduce the functional response

$$f(U)V = \beta g(U)S^* = \gamma V \frac{\beta g(U)}{\beta g(U) + \gamma}. \quad (5)$$

For monotonically increasing catch rates, the resulting functional response will also increase monotonically. Hence, dome-shaped functional responses only occur if the catch rate is not monotonically increasing.

To derive the functional response in this way and not to incorporate it directly into the model has three advantages. First, it may be easier to measure in some cases as the predation process is split up into two separate processes, i.e., searching and handling. For the conversion of searching into handling individuals, it is sufficient to introduce an entirely searching (not satiated) predator population into a prey population of different sizes to retrieve the catch rate depending on the prey population. For many experiments, that is the case anyway. However, note that one must be cautious with such measurements as a discrepancy between local measurements and a mean-field functional response, e.g., over a heterogeneous vertical water column, may exist (Morozov and Arashkevich, 2008; Morozov, 2010). Furthermore, only the time between searching events needs to be measured. Second, it shows under which assumptions a type IV functional response of the form given by Eq. (1) emerges, which will show the artificiality of this form. Third and most important for this study, it allows us to introduce a single parameter later on that changes the functional response from a saturating form into a dome-shaped form to differentiate the effect of different group defense forms from other factors.

For simplicity, we assume that the numerical response depends linearly on the functional response (for a discussion on alternatives

see Abrams and Ginzburg (2000)). In particular, this means that conversion of prey biomass into predator biomass is proportional to the predation term with a proportionality constant e , which one can interpret as conversion efficiency. Assuming that the time-scale separation is valid, this yields

$$\frac{dU}{dT} = \Phi(U) - \beta \frac{\gamma g(U)V}{\beta g(U) + \gamma}, U(0) = U_0, \tag{6a}$$

$$\frac{dV}{dT} = e\beta \frac{\gamma g(U)V}{\beta g(U) + \gamma} - mV, V(0) = V_0 \tag{6b}$$

for the original predator–prey model. Note that this form is similar to a functional response in Jeschke et al. (2002), incorporating a probability of a predator searching for prey in the classical Holling type II functional response.

This model has two stationary solutions, that always exist, i.e.,

$$E_0 = (U_0^*, V_0^*) = (0, 0), \tag{7a}$$

$$E_c = (U_c^*, V_c^*) = (K, 0). \tag{7b}$$

Depending on the growth dynamics $\Phi(U)$, more semi-trivial solutions may exist. Furthermore, depending on the form of the function $g(U)$, non-trivial solutions E_n^* may exist. These take the form

$$g(U_n^*) = \frac{m\gamma}{\beta(e\gamma - m)}, \tag{8a}$$

$$V_n^* = \frac{e\Phi(U_n^*)}{m}. \tag{8b}$$

Hence, the predator can only survive in coexistence with its prey. The function $g(U)$ is by definition a catch rate and, thus, $g(U_n^*) \geq 0$. For the existence of these solutions, this yields

$$e\gamma > m, \tag{9a}$$

$$\Phi(U_n^*) > 0. \tag{9b}$$

From a biological perspective, this means that the conversion efficiency e and the handling rate γ , which are both related to predation abilities, need to be larger than the mortality of the predator. As we assume that handling prey takes place on a shorter timescale than

birth and death processes, Eq. (9a) likely holds. Interestingly, a higher value of the searching rate β cannot compensate for lower handling rates regarding the existence of the coexistence solution.

For the linear stability of the stationary solutions, we consider the Jacobian

$$J = \begin{pmatrix} \Phi'(U) - \frac{\beta\gamma^2 g'(U)V}{(\gamma + \beta g(U))^2} & -\frac{\beta\gamma g(U)}{\gamma + \beta g(U)} \\ \frac{e\beta\gamma^2 V g'(U)}{(\gamma + \beta g(U))^2} & \frac{e\beta\gamma g(U)}{\gamma + \beta g(U)} - m \end{pmatrix}. \tag{10}$$

Evaluation at the trivial solution E_0 yields the eigenvalues $\lambda_{0,1} = \Phi'(0)$ and $\lambda_{0,2} = -m$. Hence, the trivial solution is always a saddle in absence of a strong Allee effect and a stable node in presence of a strong Allee effect.

The Jacobian evaluated at the semi-trivial solution E_c has the eigenvalues $\lambda_{c,1} = \Phi'(K)$, and $\lambda_{c,2} = \frac{\beta g(K)(e\gamma - m) - \gamma m}{\gamma + \beta g(K)}$. Hence, if no coexistence solutions exist, i.e., $e\gamma \leq m$, the semi-trivial solution is a stable node. Conversely, if coexistence is possible,

$$g(K) < \frac{m\gamma}{\beta(e\gamma - m)} = g(U_n^*). \tag{11}$$

must hold as a stability criterion. If $g(U)$ is monotonically increasing in U , this can never hold as $K > U_n^*$. However, for a non-monotonic predation rate, the carrying capacity may be stable if a coexistence solution exists. Hence, bistability between coexistence and carrying capacity may occur.

We address the stability of the coexistence solution(s) using the Routh-Hurwitz-criterion. After some simplification involving particularly Eqs. 8, one gets

$$\text{Tr}(J|_{E_n^*}) = \Phi'(U_n^*) - \kappa g'(U_n^*)\Phi(U_n^*) < 0 \tag{12a}$$

$$\det(J|_{E_n^*}) = \frac{\kappa g'(U_n^*)\Phi(U_n^*)}{m} > 0 \tag{12b}$$

with $\kappa = \frac{\beta(m - e\gamma)^2}{e\gamma^2 m}$ as conditions for stability of the coexistence solution(s). If the coexistence solution(s) exist(s), only

$$g'(U_n^*) > 0 \tag{13}$$

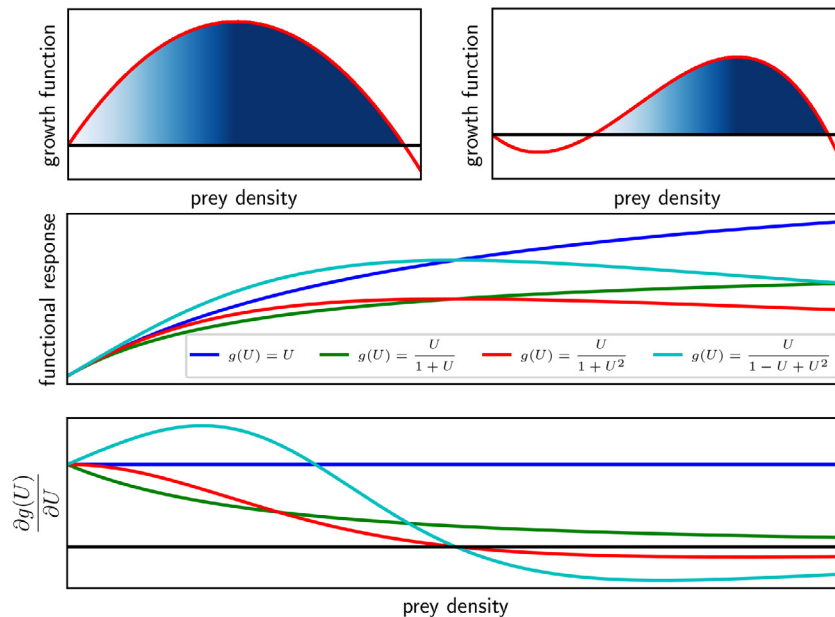


Fig. 1. A type IV functional response as in Eq. (1) overestimates stability of coexistence solutions at low prey densities. The upper panel shows logistic growth and growth with a strong Allee effect. For stability, Eqs. (12) need to hold. If $g'(U_n^*)$, shown in the lower panel, is negative, stable coexistence is not possible. If it is positive, stability is guaranteed in the dark blue regions in the upper panel. Otherwise, coexistence becomes more likely with higher $\Phi(U_n^*)$ as indicated by the blue shade and higher $g'(U_n^*)$. The panel in the middle shows the value of different functional responses $f(U)$ (ordinate) depending on the prey density. The colors indicate the underlying catch rates $g(U)$. (For interpretation of the references to colour in this figure legend, the reader is referred to the web version of this article.)

must hold for a positive determinant. Note that this is assured for a monotonically increasing catch rate. If this holds, Eq. (12a) can be rewritten as

$$\frac{\Phi'(U_n^*)}{g'(U_n^*)\Phi(U_n^*)} < \kappa. \tag{14}$$

Hence, if the conditions before hold, a sufficient condition for stability is that $\Phi'(U_n^*) < 0$. Clearly, if the coexistence state is unstable but existent in case of a monotonically increasing functional response, an asymptotically stable periodic solution must exist as the only possible stable attractor. If Eq. (13) and $Tr(J|_{E_n^*}) = 0$ hold, a Hopf bifurcation occurs (Britton, 2012). As $J_{2,2} = 0$ at the coexistence solution, the second condition requires $J_{1,1} = 0$, i.e., the bifurcation occurs at the maximum of the nontrivial prey nullcline.

From a biological perspective, the stability criterion given by Eq. (14) means that the growth function of the prey needs to be sufficiently high, i.e., $\Phi(U_n^*) \gg 0$. Furthermore, the change of the catch rate with increasing prey densities $g'(U_n^*)$ needs to be sufficiently large. To visualize this relationship, Fig. 1 shows different growth functions of the prey and different functional responses emerging from given catch rates. The figure shows five general tendencies. First, logistic growth tends to stabilize coexistence compared to a strong Allee effect (upper panel). Second, as $g'(U_n^*) > 0$ for monotonically increasing functions, the coexistence equilibrium is always stable if it exists in the dark blue regions for these functional responses. Third, the light blue line corresponds to the often used type IV functional response, cf. Eq. (1). As its derivative with respect to the prey is particularly high at low densities, it tends to overestimate the stability of the coexistence equilibrium at these densities compared to other functional responses representing group defense (red and green curve). Fourth, group defense with critical population size, i.e., a dome-shaped functional response, is more successful at high prey densities as it makes the stability of the coexistence equilibrium unlikely. Conversely, group defense leading to a saturation (green curve) is more successful for equilibria at low prey densities. Fifth, if the prey population obeys a strong Allee effect with a higher Allee threshold than the threshold of the group defense, coexistence can never be stable.

3. Model with a given catch rate

Depending on the catch rate, the resulting functional response could represent diverse biological phenomena, such as saturation, e.g., $g(U) = U$ or prey switching, e.g., $g(U) = U^2$. Here, we want to investigate the potential impact of group defense. Group defense can be represented by the catch rate

$$g(U) = \frac{U}{1 + (\frac{U}{C})^\nu}. \tag{15}$$

The form of this function is arbitrary to a certain extent. However, we will see that the shape of the functional response changes by varying ν from saturation to different dome-shaped functional responses. Most studies assume a $\nu \geq 1$. However, some studies also indicate $\nu < 1$ for species with herding behavior such as group defense (Braza, 2012). If $\nu > 1$, a dome-shaped functional response emerges while if $\nu \leq 1$, a saturating functional response emerges. If $C \gg K$, the resulting functional response coincides with the Holling type II functional response. However, if the critical value is $C < K$, it controls the impact of a higher prey density if $\nu \leq 1$. In case of $\nu > 1$, it represents a critical value beyond which the group defense has a high impact. In the following, we will refer to it as the *critical defense value*.

The derivative of this function at low densities is given by

$$\lim_{U \rightarrow 0} g'(U) = 1. \tag{16}$$

Hence, the rate of change at low densities is not affected by this function, but it impacts the shape of the curve at higher densities.

In particular,

$$\lim_{U \rightarrow \infty} g'(U) = 0 \tag{17}$$

holds at high densities. For $\nu \leq 1$, this leads to saturation of the catch rate like in the Holling type II functional response, whereas for $\nu > 1$, the catch rate has a maximum at

$$U_{max} = C(\nu - 1)^{-\frac{1}{\nu}} \tag{18}$$

meaning that higher prey densities lead to lower predation success. Even with $\nu > 1$, the model can represent different dome-shaped functional responses such as one with a linear and quadratic term (Líznarová and Pekár, 2013) or with a linear and cubic term (Tostowaryk, 1972) in the denominator.

Incorporating this function in the general model, i.e., Eq. (6), yields

$$\frac{dU}{dT} = \Phi(U) - V \frac{\beta\gamma U}{\gamma + \beta U + \gamma(U/C)^\nu}, \tag{19a}$$

$$\frac{dV}{dT} = eV \frac{\beta\gamma U}{\gamma + \beta U + \gamma(U/C)^\nu} - mV. \tag{19b}$$

It can be seen that the linear term can be neglected as in Eq. (1) only if the search rate of the predator β and handling time γ^{-1} are sufficiently small and/or if $C \ll K$. In this case, the nonlinear term in the denominator is the leading term.

Regarding the stability of the carrying capacity, we already know that it is stable if no coexistence solution exists. Otherwise, $e\gamma > m$ holds and given the functional response above

$$\frac{K}{1 + (\frac{K}{C})^\nu} < g(U_n^*) \tag{20}$$

needs to hold for stability. This demonstrates that low critical defense values and high group defense strengths increase the likelihood that the carrying capacity is stable.

Regarding the number of coexistence solutions, we can simplify Eq. (8a) to

$$U_n^{*\nu} = \frac{C^\nu}{g(U_n^*)} U_n^* - C^\nu. \tag{21}$$

Hence, a necessary condition for the existence of a coexistence solution is $U_n^* > g(U_n^*)$. Depending on ν , the potential number of stationary coexistence solutions differ. Only in the non-monotonic case, i.e., $\nu > 1$, more than one coexistence solution can exist.

In particular, if $\nu < 1$, $U_n^{*\nu}$ is a concave function. As the right hand side of Eq. (21) is a straight line intersecting the abscissa at $U = g(U_n^*) > 0$, one intersection always exists. If $\nu = 1$, the left-hand side and the right-hand side intersect at

$$U_n^* = \frac{Cg(U_n^*)}{C - g(U_n^*)}. \tag{22}$$

Hence, $C > g(U_n^*)$ needs to hold for the existence of a coexistence solution. Furthermore, $\Phi(U_n^*) > 0$ must hold for feasibility.

If $\nu > 1$, $U_n^{*\nu}$ is a convex function. Hence, either zero or two solutions exist for almost all parameter combinations satisfying $\Phi(U_n^*) > 0$. However, note that $\Phi(U_n^*) > 0$ may also just hold for one of the nontrivial solutions. In this case, the other vertical predator nullcline is at positive densities but is not biologically meaningful as it is beyond the carrying capacity. Rewriting Eq. (21) yields

$$\phi(U_n^*) = U_n^{*\nu} - \frac{C^\nu}{g(U_n^*)} U_n^{*\nu} + C^\nu = 0. \tag{23}$$

As this function has a minimum at the positive value

$$U_{nmin}^* = \sqrt[v-1]{\frac{C^v}{vg(U_n^*)}} \tag{24}$$

and $\phi(0) = C^v > 0, \phi(U_{nmin}^*) < 0$ must hold for the feasibility of two coexistence solutions. This corresponds to

$$g(U_n^*) < g(U_{n,crit}^*) = \frac{(v-1)(C^{-v}(v-1))^{-\frac{1}{v}}}{v} \tag{25}$$

At $g(U_n^*) = g(U_{n,crit}^*)$, a saddle-node bifurcation takes place. The threshold $g(U_{n,crit}^*)$ is visualized in Fig. 2. The color scale shows the maximum value of $g(U_n^*)$ for feasibility of two coexistence solutions. For higher values of C , the critical value of $g(U_n^*)$ increases monotonically. Hence, a higher critical defense value makes the feasibility of two coexistence solutions more likely. This relationship becomes more complex regarding the strength of the group defense. The function $g(U_n^*)(C, v)$ shows a minimum at $v = 2$. This corresponds to the classical function of group defense, which thus may tend to underestimate the existence of two coexistence solutions. However, note that this effect is very weak.

Now, we consider the stability of the coexistence solutions. By Eqs. (13) and (12a), we know that

$$g'(U_n^*) = \frac{C^v(C^v - (v-1)U_n^{*v})}{(C^v + U_n^{*v})^2} \tag{26}$$

is a crucial expression for the stability of the nontrivial equilibrium. In particular, a necessary condition for stability is $g'(U_n^*) > 0$, which always holds if $v \leq 1$. However, if a maximum of the catch rate exists at finite population densities, i.e., $v > 1$,

$$U_n^* < \eta(v) = \sqrt[v]{\frac{C^v}{v-1}} \tag{27}$$

must hold for stability. Note that this corresponds to the maximum of the catch rate given by Eq. (18), meaning that in case of group defense, stable coexistence is only possible at prey densities smaller than the prey density at the maximum of the catch rate. Note that this is already visualized in Fig. 1. From this condition, we can see Appendix (B) that

$$\lim_{v \rightarrow \infty} \eta(v) = C \tag{28}$$

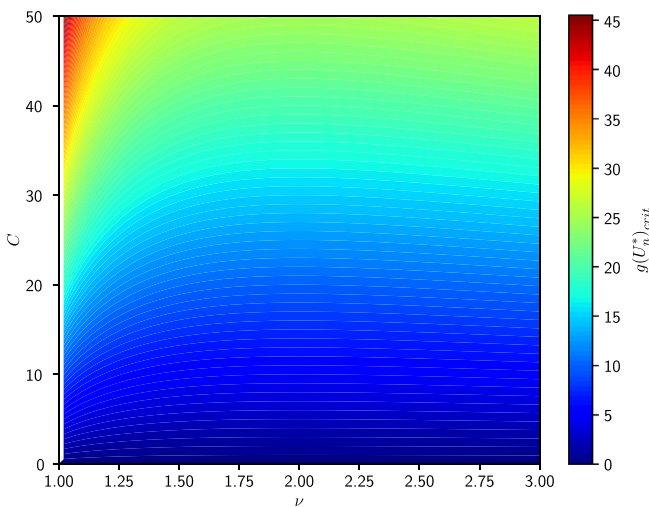


Fig. 2. The likelihood of the feasibility of a second coexistence solution tends to increase with a higher critical defense value and higher group defense strength. The threshold $g(U_{n,crit}^*)$ given by Eq. (25) is visualized. Low values denoted by blue colors correspond to situations in which the feasibility of two coexistence solutions is unlikely. Note that for $v \leq 1$, two coexistence solutions are never possible.

and

$$\lim_{v \rightarrow 1^+} \eta(v) = \infty. \tag{29}$$

Furthermore, for $v = 2, \eta(v) = C$ holds. Hence, for high group defense values as well as for $v = 2$, prey and predator can only coexist at values $U_n^* < C$ underlining the criticality of this parameter. There is no biologically meaningful threshold close to saturation of the catch rate. Note that this is only a necessary condition for stability. As a sufficient condition, $g'(U)$ needs to be sufficiently large. It is obvious that

$$g''(U_n^*) = -\frac{vC^v U_n^{*v-1}((1+v)C^v - (v-1)U_n^{*v})}{(C^v + U_n^{*v})^3} \tag{30}$$

is negative if $v \leq 1$. Furthermore, if $v > 1, g''(U_n^*)$ is negative if

$$U_n^{*v} < \frac{(1+v)C^v}{v-1}. \tag{31}$$

As

$$\frac{C^v}{v-1} < \frac{(1+v)C^v}{v-1}, \tag{32}$$

one can say from Eq. (27) that $g'(U_n^*)$ is a monotonically decreasing function in U_n^* as long as $g'(U_n^*)$ is positive. Thus, with smaller values of U_n^* , stability of the equilibrium gets more likely. However, in these regions, stable coexistence is unlikely due to the growth functions (see Fig. 1). In particular, if a strong Allee effect is present, this makes coexistence unlikely as $\Phi(U_n^*) > 0$ needs to hold as well. Hence, a strong Allee effect prevents stable coexistence at low densities while group defense prevents stable coexistence at high densities. Thus, a combination of a strong Allee effect in the prey and group defense may be detrimental for predators.

Table 1 summarizes the feasibility and stability conditions of model (19).

For the numerical investigation of the model, we have chosen a logistic growth function

$$\Phi(U) = rU - cU^2 \tag{33}$$

where rc^{-1} represents the carrying capacity K . Fig. 3 shows a bifurcation diagram for the two parameters representing the group defense. For the remaining parameters, we used estimations based on an ecological microtine rodent mustelid model from Huisman and De Boer (1997) and Hanski and Korpimäki (1995) satisfying the conditions for timescale separation, see Appendix A. The usage of this case study makes sense as rodents show anti-predator behavior such as ultrasonic vocalizations as an alarm signal that can be interpreted as group defense (Blanchard et al., 1990).

C is the critical defense value, while v shapes the form of the functional response. Recall that for high C , the functional response tends to the Holling type II functional response. Hence, it is evident, that group defense is beneficial for the prey as it increases the likelihood that the carrying capacity is the only stable stationary solution.

At higher values of v or low values of C , the carrying capacity of the prey is the only stable stationary solution. Hence, it is evident that stronger group defense is beneficial for the prey population for most parameter regions. Note that the exact values of v and C depend on the parameter set. The values stated in the following are just for reference regarding Fig. 3. For $v \lesssim 1.4$, a stable coexistence solution emerges for high values of C via a transcritical (solid black line) bifurcation. Increasing the value of C even further, this equilibrium undergoes a Hopf bifurcation (blue line), leading to a limit cycle. For $v \gtrsim 1.4$, this limit cycle vanishes via a homoclinic bifurcation (dashed line) for sufficiently low C . This homoclinic bifurcation coincides with a transcritical bifurcation. Fig. C.7

Table 1

Feasibility and stability of solutions for model (19) assuming that $\Phi(U) = 0$ only at $U = 0$ and $U = K$, i.e., in absence of a strong Allee effect.

Solution	Feasibility	Stability
$(U_0, V_0) = (0, 0)$	unconditionally feasible	unconditionally unstable
$(U_c, V_0) = (K, 0)$	unconditionally feasible	if $e\gamma \leq m$ or if $g(K) < g(U_n^*)$
$(U_{n,1}, V_{n,1})$	nec.: $U_n^* > g(U_n^*)$	nec.: if $v \leq 1$ or if $v > 1 \wedge U_{n,1} < \sqrt{\frac{e\gamma}{v-1}}$
$(U_{n,2}, V_{n,2})$	$v > 1 \wedge g(U_n^*) < g(U_n^*)_{crit}(C, v) \wedge \Phi(U_n^*) > 0$	nec.: $U_{n,2} < \sqrt{\frac{e\gamma}{v-1}}$

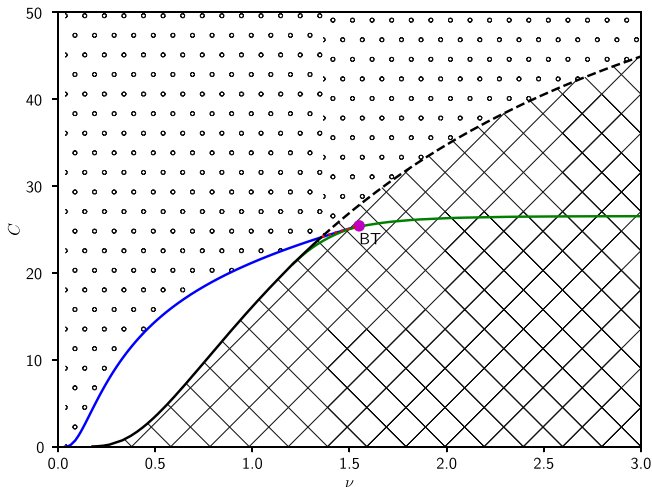


Fig. 3. Group defense can lead to extinction of the predator. A two-dimensional bifurcation diagram with v , and the critical defense value C as bifurcation parameters is shown. In the squared region, the prey exists at its capacity. The solid black line corresponds to a transcritical bifurcation leading to a stable coexistence state (white region). This stable coexistence state loses stability via a Hopf bifurcation (blue line), resulting in a stable limit cycle (dotted area). For higher v , the limit cycle is destroyed via a homoclinic bifurcation that takes place simultaneously with a transcritical bifurcation (dashed black line). Note that between green, blue, and black solid lines, the system is bistable. It depends on the initial conditions, whether the system converges to the stable coexistence state or the carrying capacity of the prey. BT indicates the Bogdanov-Takens bifurcation point. From this point, a homoclinic bifurcation (red dotted line) emerges. Below this line, a small parameter region corresponding to bistability between a limit cycle and the carrying capacity exists. The remaining parameters are as stated in A. We computed the bifurcation curves using XPPAUT (Ermentrout, 2002). (For interpretation of the references to color in this figure legend, the reader is referred to the web version of this article.)

illustrates the homoclinic orbit. Furthermore, for $v > 1$, i.e., if group defense is dome-shaped, a saddle-node bifurcation exists (green line). However, note that we have only plotted the saddle-node bifurcation in the parameter regions in which it takes place at biologically meaningful densities. Furthermore, note that the green line corresponds to a particular isocline of Fig. 2. Hence, it has a maximum value $v = 2$.

Note that bifurcations have been extensively studied for predator-prey models with Holling type II functional response as well as with type IV functional response. However, this bifurcation diagram allows seeing the impact of defense directly. In particular, if C is sufficiently low, i.e., $C \lesssim 16.1$, a saturating group defense functional response is sufficient. In this case, the carrying capacity is the only stable solution already at $v = 1$ corresponding to a saturating functional response. For values higher than this threshold, group defense makes leading to a non-monotonic functional response makes sense as it may turn the carrying capacity into a stable equilibrium via a transcritical bifurcation. However, at high values of C , corresponding to high critical defense values, the tran-

sritical bifurcation curve (and the homoclinic bifurcation curve) tends to saturate. In this case, group defense does not change the system dynamics. As already stated above, for very large values of C , the functional response converges to the Holling type II functional response. Hence, from the bifurcation diagram, it is evident that group defense, in general (independent of the exact form), has the potential to drive the predator to extinction.

On the left-hand side of the Bogdanov-Takens bifurcation, bistability can occur. As the parameter regions corresponding to bistability are very small, Fig. 4 shows a sketch of this region. It demonstrates that above the saddle-node bifurcation, bistability can occur either with one stationary coexistence state and the carrying capacity. This is a phenomenon that only occurs for a non-monotonic functional response. Hence, catch rates with a critical value increase the complexity of the model. Furthermore, in a small parameter region, a paradox can occur. On the left-hand side and above of the red dotted homoclinic bifurcation curve, the capacity is the only stable stationary solution. Increasing the strength of collective defense by increasing v or decreasing the critical value C , the system becomes bistable. In this case, a stable limit cycle or a stable stationary coexistence state exists. Fig. 5 shows such a transition as an illustration of this paradox. At low critical defense values, the system is bistable in this case. Starting in the region separated by the stable manifold, the system converges to a limit cycle. Increasing the value of C which can be interpreted as decreasing the collective defense efficacy leads to an increase in the amplitude of the predator-prey oscillations. At some point

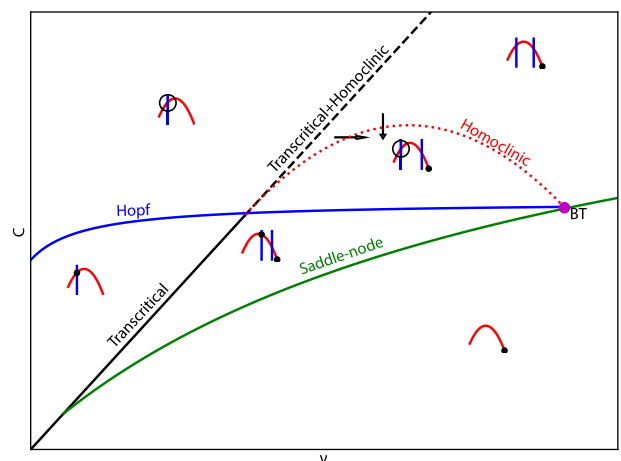


Fig. 4. In case of a non-monotonic functional response, group defense can lead to complex dynamics including a paradox. A sketch of the region around the Bogdanov-Takens bifurcation in Fig. 3 is shown. The small plots represent sketches of the phase plane. Circles denote stable limit cycles; the black dots represent stable equilibria. Note that for convenience, we did not show the trivial nullclines. The paradox is visualized by the arrows. Here, increasing the group defense by increasing v or decreasing C can prevent the predator from extinction.

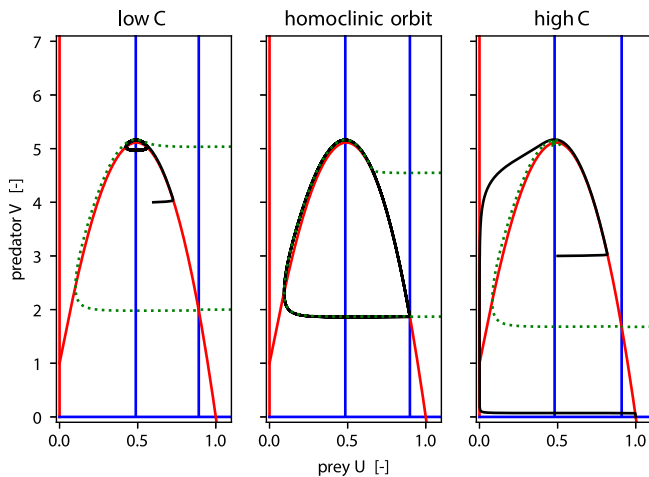


Fig. 5. Increasing the critical defense value can drive the predator to extinction. The phase plane for three different parameter combinations are shown to illustrate the paradox. Black lines are sample trajectories, blue and red lines represent predator and prey nullclines, respectively. The dotted green lines represents the stable manifold of the saddle (right coexistence state). Parameters are $v = 1.38$, $C_{low} = 24.3$, $C_{homoclinic} \approx 24.32$, $C_{high} = 24.35$. The remaining parameters are as stated in A. (For interpretation of the references to color in this figure legend, the reader is referred to the web version of this article.)

the limit cycle vanishes via a homoclinic bifurcation. The homoclinic orbit is shown in the middle panel. Without the stable limit cycle, the system is monostable and every initial condition converges to the prey carrying capacity. Hence, increasing the critical defense value is beneficial for the prey in this case. The same can happen with an increase of the defense strength v .

4. Discussion and conclusion

In this study, we proposed a functional response incorporating group defense based on timescale separation arguments. Here, a dome-shape may or may not emerge. In particular, if the catch rate increases monotonously with increasing prey density, the resulting functional response is also a saturating function, although it incorporates group defense. However, compared to the Holling type II functional response, the saturation value is lower. We provided an example for that, cf. green curve in Fig. 1. Group defense that is not leading to a dome-shaped functional response is commonly found in experiments (Jeschke and Tollrian, 2005; Olson et al., 2013). Thus, with our approach, we obtain a class of group defense functional responses that can represent at least two biologically meaningful shapes. Hence, with the derivation, we also underpin the idea that group defense is likely to be present in many systems, although not clearly indicated by the measured functional response (Jeschke and Tollrian, 2005).

The dome-shaped functional response emerges only if a critical prey density exists beyond which the catch rate decreases again, cf. the red curve in the lower panel of Fig. 1. This is a valuable finding as the mechanisms leading to dome-shaped functional responses are not fully understood for some systems (Mezzalana et al., 2017).

From a modeling perspective, we have shown that the type IV functional response, as in Eq. (1), potentially overestimates stable coexistence at low prey densities. If the prey population exists at low densities, the type IV functional response without linear prey dependence in the denominator seems to be a good approximation. However, we have shown that the linear term in the denominator is only negligibly small if the searching rate and the handling time are low and/or the critical defense value is much lower than the carrying capacity of the prey. This is a strong assumption for many predator-prey relationships. Indeed, some ecological studies even

lead to the conclusion that the linear component in the denominator in the functional response is much more pronounced than the quadratic component (Líznavá and Pekár, 2013). If this is not clear, a functional response, as proposed in this study, should preferably be used.

For a saturating functional response, only one nontrivial equilibrium can exist, while for a dome-shaped functional response, up to two coexistence equilibria can occur. This allows for the possibility of a homoclinic bifurcation in the model and increases the complexity of the behavior in general. Regarding the stability of coexistence, a strong Allee effect in the prey combined with a dome-shaped functional response shrinks the interval of the prey density in which stable coexistence is possible. Furthermore, we have applied bifurcation analysis for the defense parameters showing that group defense increases the extinction probability of the predator. However, for low critical defense values, a saturating functional response is sufficient as the carrying capacity of the prey is the only stable attractor. The same holds for very high critical defense values. In this case, group defense does not have a qualitative impact and should thus be omitted if it is related to costs.

Finally, we have shown that for a small range of parameters, a paradox can occur. Lowering the critical defense value or increasing the strength of the group defense gives rise to stable coexistence (either stationary or oscillatory) that is not possible at slightly higher critical defense value or lower strength of the group defense. However, it needs further investigations to know whether this paradox can occur over larger parameter regimes and thus would have ecological relevance.

CRediT authorship contribution statement

Merlin C. Köhnke: Conceptualization, Methodology, Software, Validation, Formal analysis, Writing - original draft, Writing - review & editing, Visualization. **Ivo Siekmann:** Conceptualization, Methodology, Supervision, Writing - review & editing. **Hiromi Seno:** Conceptualization, Methodology, Supervision, Writing - review & editing. **Horst Malchow:** Methodology, Supervision, Writing - review & editing.

Declaration of Competing Interest

The authors declare that they have no known competing financial interests or personal relationships that could have appeared to influence the work reported in this paper.

Acknowledgments

The Japan Society for the Promotion of Science (JSPS) that provided funding for a stay at Tohoku University for MCK and HM supported this work. MCK acknowledge discussions with Frank M. Hilker about the bifurcation analysis.

Appendix A. Timescale separation

One necessary assumption for the validity of the timescale separation is that birth and death processes happen on another timescale compared to other processes such as predation or competition. In particular, following Segel (1988), we can find a characteristic timescale for the processes described by Eq. (3). Assuming that changes in U and V are sufficiently small compared to changes in S and H , we set $U = U_0$ and $V = V_0$ and rewrite Eq. (3a) yielding

$$\frac{dS}{dt} = -(\beta g(U_0) + \gamma) \left(S - \frac{\gamma V_0}{\beta g(U_0) + \gamma} \right). \quad (\text{A.1})$$

In this form, the stationary solution, as well as the characteristic timescale $t_s = \Gamma^{-1} = (\gamma + \beta g(U_0))^{-1}$ is directly visible. If l is large compared to the vital parameters of the populations, U and V do not change significantly in this time, and the timescale separation is valid. In particular, this approach illustrates that the parameters β and γ need to be large compared to the magnitude of $\Phi(U)$ and m representing birth and death processes.

More specifically, this holds if the upper bound of the flow per characteristic time interval is significantly small. An approximation for this is given by

$$\max \left(\left| t_s \frac{dU}{dT} \right|_{|_{max}}, \left| t_s \frac{dV}{dT} \right|_{|_{max}} \right) \ll \Upsilon. \quad (\text{A.2})$$

Here, Υ depends on the order of magnitude of the state variables. Note that this is just an estimation as the flow may be changing in the time interval $[t, t + t_s]$. However, as the flow depends continuously on the state variables and the time interval is small, this estimate will give a reasonable value.

To investigate whether the timescale separation is valid, we use a logistic growth function and parameterize the model with the same two parameter sets as in Huisman and De Boer (1997). In particular, they use one parameter set from Scheffer and De Boer (1995) corresponding to an algae zooplankton model and one parameter set from Hanski and Korpimäki (1995) corresponding to a microtine rodent mustelid model. As our functional response looks slightly different from the classical Holling type II functional response, we estimate the parameters β and γ with a Gradient method, see, e.g., Polak (2012).

The adjusted parameters for the algae zooplankton model are $r = 0.5 \text{ day}^{-1}$, $c = 0.05 \text{ l (day mg DW)}^{-1}$, $e = 0.6$, $\beta = 0.67 \text{ l (day mg DW)}^{-1}$, $\gamma = 0.4 \text{ day}^{-1}$, $m = 0.15 \text{ day}^{-1}$. If either the equation for the prey or the predator changes significantly, the timescale separation approach is not valid. For convenience, we let $V \rightarrow 0$ and examine only $|\Phi(U)t_s|$ depending on the exact form of $g(U)$. This is a biologically relevant parameter choice as it may correspond to a predator invading into a habitat with only prey. Fig. A.6a shows the dependence on the density of the prey and on v . It can be seen that the quasi-steady-state assumption does

not hold for this parameter set for most values of U . Furthermore, higher values of v tend to increase the length of the time interval and thus make the quasi-steady-state assumption even worse. Note that a reason for the failure of the timescale separation may be the short lifespan of microorganisms. This becomes directly apparent, comparing the intrinsic death rate m with the predation parameters β and γ .

The adjusted parameters for the rodent mustelid model are $r = 4.05 \text{ year}^{-1}$, $c = 0.054 \text{ ha (individuals year)}^{-1}$, $e = 0.0023$, $\beta = 118.7 \text{ ha (individuals year)}^{-1}$, $\gamma = 600.7 \text{ year}^{-1}$, $m = 1 \text{ year}^{-1}$. In this case, the rate of change of the growth function is comparably low (Fig. A.6b). Note that in the predation terms, the validity does not only depend on one species but on both species. However, for relevant combinations of U and V , i.e., combinations with densities that are realistic in the phase plane, the timescale separation still holds in this case. As before, higher values of v tend to increase the rate of change. However, for the predation term, this only holds until a maximum of $v \approx 2$. Beyond this threshold, the function is decreasing again. Nevertheless, in models without group defense, the validity of the timescale separation seems to be more likely.

Appendix B. Limit of $\eta(v)$

$$\begin{aligned} \lim_{v \rightarrow \infty} \sqrt{\frac{C^v}{v-1}} &= \lim_{v \rightarrow \infty} \exp \ln \sqrt{\frac{C^v}{v-1}} \\ &= \lim_{v \rightarrow \infty} \exp \frac{\ln C^v}{\sqrt{v-1}} \\ &= \exp \lim_{v \rightarrow \infty} \frac{\ln C^v - \ln(v-1)}{v} \end{aligned}$$

The numerator grows asymptotically slower than v , thus $\lim_{v \rightarrow \infty} \frac{\ln(v-1)}{v} = 0$. Furthermore, as $\ln C^v / v = v \ln C / v = \ln C$, $\lim_{v \rightarrow \infty} \sqrt{\frac{C^v}{v-1}} = C$ holds.

Appendix C. Homoclinic orbit

Fig. C.7 illustrates a sample trajectory close to the homoclinic orbit that coincides with the transcritical bifurcation. At the transcritical bifurcation, the right predator nullcline gives rise to a second coexistence equilibrium.

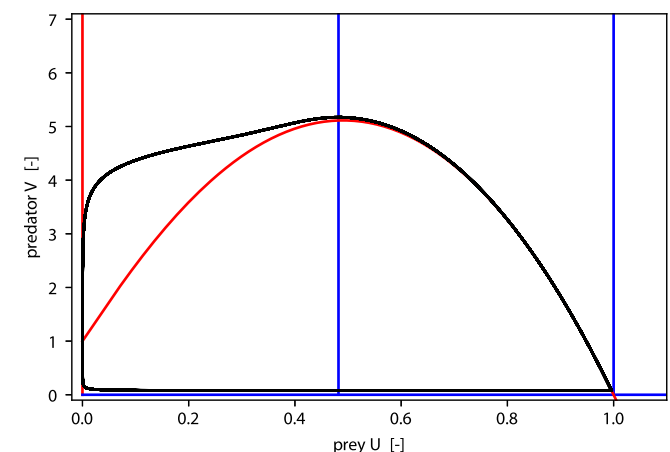


Fig. C.7. The homoclinic orbit destroying the limit cycle in the monostable case coincides with a transcritical bifurcation. The phase plane for three different parameter combinations are shown to illustrate the paradox. The black line is a sample trajectory close to the homoclinic orbit, blue and red lines represent predator and prey nullclines, respectively. Parameters are $v = 1.36$ and $C = 24.2$. The remaining parameters are as stated in A. (For interpretation of the references to color in this figure legend, the reader is referred to the web version of this article.)

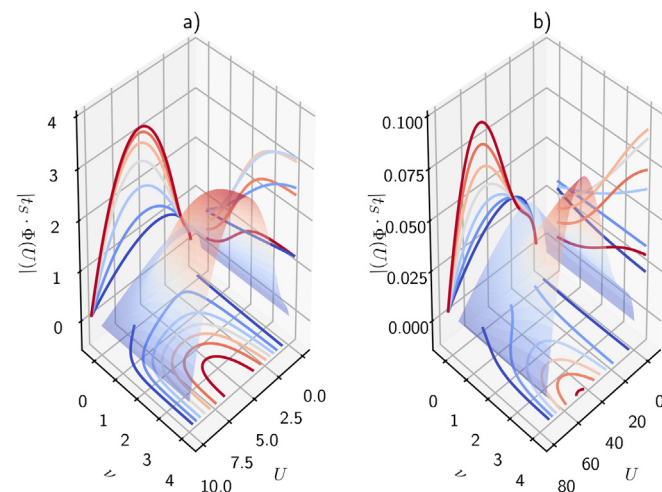


Fig. A.6. For the algae zooplankton model, the timescale separation is not valid while it is valid for the rodent mustelid model. The expression $z = |\Phi(U)t_s|$ is plotted for different defense strengths v and different population sizes of the prey U . The right panel refers to the rodent mustelid model. In this case, the steady-state assumption is valid based on this expression, while it is not valid for the zooplankton model (left panel). Furthermore, it can be seen (contours in the U, z -plane) that stronger group defense make the validity of the quasi-steady-state assumption less likely while it seems to be most likely for low or high prey densities.

References

- Abrams, P.A., Ginzburg, L.R., 2000. The nature of predation: prey dependent, ratio dependent or neither? *Trends in Ecology & Evolution* 15 (8), 337–341.
- Aldebert, C., Nerini, D., Gauduchon, M., Poggiale, J., 2016. Structural sensitivity and resilience in a predator–prey model with density-dependent mortality. *Ecological Complexity* 28, 163–173.
- Allan, J.D., 1995. Predation and its consequences. In: *Stream Ecology*. Springer, pp. 163–185.
- Allee, W., 1958. *The Social Life of Animals*. .
- Andrews, J.F., 1968. A mathematical model for the continuous culture of microorganisms utilizing inhibitory substrates. *Biotechnology and Bioengineering* 10 (6), 707–723.
- Baek, H., 2010. A food chain system with Holling type IV functional response and impulsive perturbations. *Computers & Mathematics with Applications* 60 (5), 1152–1163.
- Blanchard, R.J., Blanchard, D.C., Rodgers, J., Weiss, S.M., 1990. The characterization and modelling of antipredator defensive behavior. *Neuroscience & Biobehavioral Reviews* 14 (4), 463–472.
- Blanchard, R.J., Flannelly, K.J., Blanchard, D.C., 1986. Defensive behaviors of laboratory and wild *Rattus norvegicus*. *Journal of Comparative Psychology* 100 (2), 101.
- Bodenstein, M., 1913. Eine Theorie der photochemischen Reaktionsgeschwindigkeiten. *Zeitschrift für physikalische Chemie* 85 (1), 329–397.
- Braza, P.A., 2012. Predator–prey dynamics with square root functional responses. *Nonlinear Analysis: Real World Applications* 13 (4), 1837–1843.
- Britton, N.F., 2012. *Essential Mathematical Biology*. Springer Science & Business Media.
- Caro, T., 2005. *Antipredator Defenses in Birds and Mammals*. University of Chicago Press.
- Chen, Y., 2004. Multiple periodic solutions of delayed predator–prey systems with type IV functional responses. *Nonlinear Analysis: Real World Applications* 5 (1), 45–53.
- Collings, J.B., 1997. The effects of the functional response on the bifurcation behavior of a mite predator–prey interaction model. *Journal of Mathematical Biology* 36 (2), 149–168.
- Diekmann, O., Heesterbeek, H., Britton, T., 2012. *Mathematical Tools for Understanding Infectious Disease Dynamics*, vol. 7. Princeton University Press.
- Edmunds, M., 1974. *Defence in Animals: A Survey of Anti-Predator Defences*. Longman Publishing Group.
- Edwards, V.H., 1970. The influence of high substrate concentrations on microbial kinetics. *Biotechnology and Bioengineering* 12 (5), 679–712.
- Ermentrout, B. (2002). *Simulating, analyzing, and animating dynamical systems: a guide to XPPAUT for researchers and students*, vol. 14. Siam..
- Fujii, K., Holling, C., Mace, P., 1986. A simple generalized model of attack by predators and parasites. *Ecological Research* 1 (2), 141–156.
- Gross, T., Ebenhöf, W., Feudel, U., 2004. Enrichment and foodchain stability: the impact of different forms of predator–prey interaction. *Journal of Theoretical Biology* 227 (3), 349–358.
- Hanski, I., Korpimäki, E., 1995. Microtine rodent dynamics in northern Europe: parameterized models for the predator–prey interaction. *Ecology* 76 (3), 840–850.
- Holling, C., 1961. Principles of insect predation. *Annual Review of Entomology* 6 (1), 163–182.
- Holling, C.S., 1959. The components of predation as revealed by a study of small-mammal predation of the European pine sawfly. *The Canadian Entomologist* 91 (5), 293–320.
- Huang, J.-C., Xiao, D.-M., 2004. Analyses of bifurcations and stability in a predator–prey system with Holling type-IV functional response. *Acta Mathematicae Applicatae Sinica* 20 (1), 167–178.
- Huisman, G., De Boer, R.J., 1997. A formal derivation of the 'Beddington' functional response. *Journal of Theoretical Biology* 185 (3), 389–400.
- Ivlev, V.S., 1961. *Experimental Ecology of the Feeding of Fishes*. Yale University Press, New Haven.
- Jeschke, J.M., 2006. Density-dependent effects of prey defenses and predator offenses. *Journal of Theoretical Biology* 242 (4), 900–907.
- Jeschke, J.M., Kopp, M., Tollrian, R., 2002. Predator functional responses: discriminating between handling and digesting prey. *Ecological Monographs* 72 (1), 95–112.
- Jeschke, J.M., Tollrian, R., 2000. Density-dependent effects of prey defences. *Oecologia* 123 (3), 391–396.
- Jeschke, J.M., Tollrian, R., 2005. Effects of predator confusion on functional responses. *Oikos* 111 (3), 547–555.
- Klump, G., Shalter, M., 1984. Acoustic behaviour of birds and mammals in the predator context; I. Factors affecting the structure of alarm signals. II. The functional significance and evolution of alarm signals. *Zeitschrift für Tierpsychologie* 66 (3), 189–226.
- Köhnke, M., 2019. Invasion dynamics in an intraguild predation system with predator-induced defense. *Bulletin of Mathematical Biology* 81 (10), 3754–3777.
- Krams, I., Bērziņš, A., Krama, T., 2009. Group effect in nest defence behaviour of breeding pied flycatchers, *Ficedula hypoleuca*. *Animal Behaviour* 77 (2), 513–517.
- Lainhart, W., Stolfa, G., Koudelka, G.B., 2009. Shiga toxin as a bacterial defense against a eukaryotic predator, *Tetrahymena thermophila*. *Journal of Bacteriology* 191 (16), 5116–5122.
- Lass, S., Spaak, P., 2003. Chemically induced anti-predator defences in plankton: a review. *Hydrobiologia* 491 (1–3), 221–239.
- Lian, F., Xu, Y., 2009. Hopf bifurcation analysis of a predator–prey system with Holling type IV functional response and time delay. *Applied Mathematics and Computation* 215 (4), 1484–1495.
- Liznarová, E., Pekár, S., 2013. Dangerous prey is associated with a type 4 functional response in spiders. *Animal Behaviour* 85 (6), 1183–1190.
- Mezzalana, J.C., Bonnet, O.J., Carvalho, P.C., 2017. D. F., Fonseca, L., Bremm, C., Mezzalana, C.C., and Laca, E.A. Mechanisms and implications of a type IV functional response for short-term intake rate of dry matter in large mammalian herbivores. *Journal of Animal Ecology* 86 (5), 1159–1168.
- Morozov, A., Arashkevich, E., 2008. Patterns of zooplankton functional response in communities with vertical heterogeneity: a model study. *Mathematical Modelling of Natural Phenomena* 3 (3), 131–148.
- Morozov, A.Y., 2010. Emergence of Holling type III zooplankton functional response: bringing together field evidence and mathematical modelling. *Journal of Theoretical Biology* 265 (1), 45–54.
- Olson, R.S., Hintze, A., Dyer, F.C., Knoester, D.B., Adami, C., 2013. Predator confusion is sufficient to evolve swarming behaviour. *Journal of The Royal Society Interface* 10 (85), 20130305.
- Pekár, S., 2005. Predatory characteristics of ant-eating Zodarion spiders (Araneae: Zodarionidae): potential biological control agents. *Biological Control* 34 (2), 196–203.
- Polak, E., 2012. *Optimization: Algorithms and Consistent Approximations*, vol. 124. Springer Science & Business Media.
- Scheffer, M., De Boer, R.J., 1995. Implications of spatial heterogeneity for the paradox of enrichment. *Ecology* 76 (7), 2270–2277.
- Segel, L.A., 1988. On the validity of the steady state assumption of enzyme kinetics. *Bulletin of Mathematical Biology* 50 (6), 579–593.
- Shoffner, S., Schnell, S., 2017. Approaches for the estimation of timescales in nonlinear dynamical systems: Timescale separation in enzyme kinetics as a case study. *Mathematical Biosciences* 287, 122–129.
- Sokol, W., Howell, J., 1981. Kinetics of phenol oxidation by washed cells. *Biotechnology and Bioengineering* 23 (9), 2039–2049.
- Tener, J., 1965. *Muskoxen*. Queen's Printer, Ottawa.
- Tostowaryk, W., 1972. The effect of prey defense on the functional response of *Podisus modestus* (Hemiptera: Pentatomidae) to densities of the sawflies *Neodiprion swainaei* and *N. pratti banksianae* (Hymenoptera: Neodiprionidae). *The Canadian Entomologist* 104 (1), 61–69.
- Upadhyay, R.K., Raw, S.N., 2011. Complex dynamics of a three species food-chain model with Holling type IV functional response. *Nonlinear Analysis: Modelling and Control* 16 (3), 353–374.
- Wang, Q., Dai, B., Chen, Y., 2009. Multiple periodic solutions of an impulsive predator–prey model with Holling-type IV functional response. *Mathematical and Computer Modelling* 49 (9–10), 1829–1836.
- Zhang, S., Tan, D., Chen, L., 2006. Chaos in periodically forced Holling type II predator–prey system with impulsive perturbations. *Chaos, Solitons & Fractals* 28 (2), 367–376.